Supplementary Information

Engineering COFs as Smart Triggers for Rapid Capture and Controlled Release of Singlet Oxygen

Dong Yan,[a,b] En Lin, [a,b] Fazheng Jin, [a,b] Shan Qiao,[c] Yi Yang, [a,b] Zhifang Wang, [a,b] Fanhao Xiong, [a,b] Yao Chen,[c] Peng Cheng [a,b,d] and Zhenjie Zhang* [a,b,c,d]

1. Detailed experimental section

1.1 Synthesis of the linkers

1.1.1 Synthesis of 4,4'-(anthracene-9,10-diyl)dianiline (ANT)

4,4'-(anthracene-9,10-diyl)dianiline (ANT) was synthesized according to a previously published procedure with slight modification.[1]

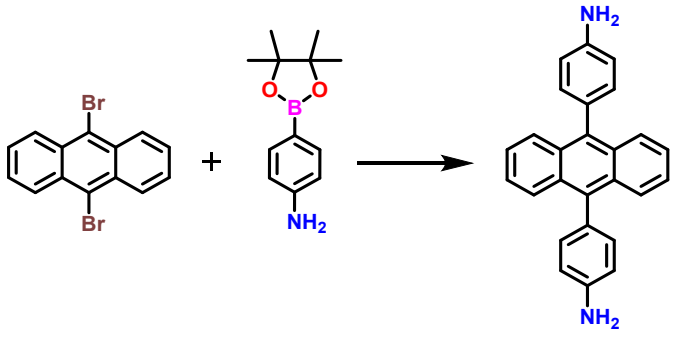

ANT

4,4'-(anthracene-9,10-diyl)dianiline (ANT). A mixture of 9,10-dibromoanthracene (1 g, 3 mmol), 4-aminophenylboronic acid pinacol ester (1.64 g, 7.5 mmol,) and Na_2CO_3 (640 mg, 6 mmol) in Dioxane/H_2O (4:1, 100 mL) was degassed with nitrogen for 15 minutes. $Pd(PPh_3)_4$ (320 mg, 0.28 mmol) was added to the mixture and heated at 110 °C for 48 h under nitrogen. The reaction mixture was filtered through a celite column to remove the palladium salt and the filtrate was diluted with ethanol. Then the product was crystallized after the organic layers cooled and later stood for 30 min. Then the yellow solid was collected, and filtered, and then washed with hexane. Yield: 584 mg (58.4 %). ^{1}H-NMR (400 MHz, chloroform-*d*) δ 7.8 (m, 4H), 7.31 (m, 4H), 7.24 (d, 4H), 6.92 (d, 4H), 3.71 (s, 4H).

1.1.2 Synthesis of 2,2',7,7'-tetramethoxy-9,9'-spirobi[fluorene]-3,3',6,6'-tetracarbaldehyde (TMSFTA).

TMSFTA was synthesized according to a previously published procedure with slight modification.[2]

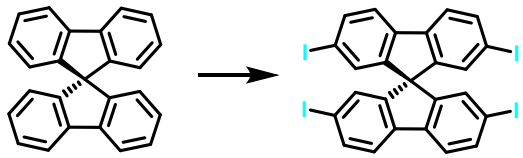

a

Synthesis of 2,2',7,7'-tetraiodo-9,9'-spirobifluorene (a). In a 250 mL two-necked flask with a reflux condenser and drying tube, 9,9'-spirobifluorene (6.32 g, 20.0 mmol) was dissolved in 60 mL of chloroform at room temperature before iodine (11.6 g, 45.6 mmol) and bis(trifluoroacetoxy)iodobenzene (21.5 g, 50.0 mmol) were added successively. After stirring for 2 hours, the product was filtered, washed with chloroform, and dried in an oven at 60 °C. The chloroform solutions were combined and washed in succession with a saturated sodium sulfite solution, saturated sodium carbonate solution, and water. After drying over $MgSO_4$, this solution was evaporated and a second product fraction was obtained. Both product fractions were combined and boiled in acetone. Compound **a** was obtained after filtering as a colorless powder (12.8 g, 78 %). ^{1}H NMR (400 MHz, chloroform-*d*) δ 7.72 (d, 4H), 7.56 (d, 4H), 7.00 (d, 4H).

Synthesis of 2,2',7,7'-Tetramethoxy-9,9'-spirobifluorene (b).

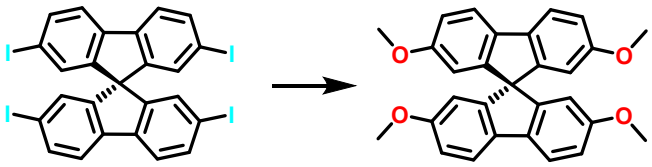

b

2,2',7,7'-Tetramethoxy-9,9'-spirobifluorene (b). To a solution of compound **a** (3 g, 3.7 mmol) in dry DMF (40 mL). sodium methoxide (9 g, 166.7 mmol) was dissolved in HPLC grade methanol (40 mL) and 80 mL anhydrous DMF. The mixture was sonicated for 10 min until the solution became homogeneous. Then the solution was added dropwise and solid CuI (0.7 g, 3.65 mmol) was added. The mixture was heated at 100°C under argon for 12 h. The resulting suspension was cooled at room temperature, diluted with water (100 mL), and acidified with 2 M HCl to pH = 1. The resulting precipitate was filtered and purified by flash chromatography with PE/EA (5/1) to afford pure compound **b** as white solid (2 g, 62.5%). ^{1}H NMR (400 MHz, chloroform-*d*) δ 7.62 (d, 4H), 6.88 (d, 4H), 6.24 (d, 4H), 3.64 (s, 12H).

Synthesis of (TMSFTA). 2,2',7,7'-Tetramethoxy-9,9'-spirobifluorene (**b)** (0.64 g, 1.468 mmol) in dry dichloromethane (50 mL) was placed, under argon flow, in a three-neck round-bottom flask connected to two drying tubes, and cooled at -10ºC. A solution of titanium tetrachloride (5.57 g, 29.36 mmol) in dichloromethane (20 mL) was added dropwise. The mixture was stirred at -10ºC for 30 min. α, α - dichloromethylmethylether (2.68 g, 23.36 mmol) was subsequently added dropwise to the reaction mixture. The reaction was stirred for 3 hours at -10 ºC and then allowed to warm at r.t. overnight. The resulting suspension was cooled at 0ºC, diluted with water (50 mL), and acidified with 2 M HCl to pH = 1. The two layers were separated and the aqueous phase was extracted with EA (50 mL). The organic phases were washed with saturated aqueous $NaHCO_3$ and brine. The solution was dried over $MgSO_4$ and the solvent was removed under reduced pressure. The resulting brown solid was purified through flash chromatography with the DCM/EA (9/1) to afford the product (0.6 g, 75%) as the white solid. ^{1}H NMR (600 MHz, chloroform-*d*) δ 10.49 (s, 4H), 8.30 (s, 4H), 6.29 (s, 4H), 3.72 (s, 12H);

1.1.3 Synthesis of 1,3,6,8-tetrakis(4-aminophenyl) pyrene (Py)

1,3,6,8-tetrakis(4-aminophenyl) pyrene (**Py**) was synthesized according to the literature with slight modification. [3]

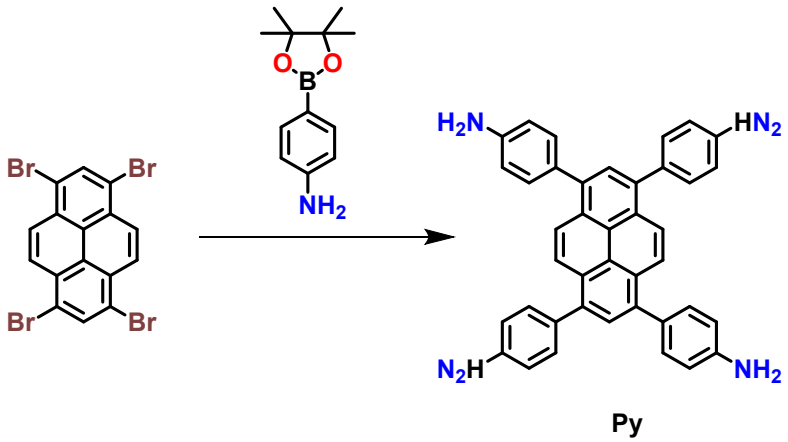

Py

1,3,6,8-tetrakis(4-aminophenyl) pyrene (Py). 1,3,6,8-tetrabromopyrene (5 g, 9.66 mmol), 4-aminophenyl boronic acid pinacol ester (10.13 g, 46.28 mmol), K_2CO_3 (7.43 g, 53.38 mmol), and $Pd(PPh_3)_4$ (1.11 g, 0.97 mmol) were introduced into a mixture of 1,4-dioxane (200 mL) and H_2O (35 mL). The resulting mixture was refluxed at 115 °C under an N_2 atmosphere for 3 days. After cooling to room temperature, the solution was poured into water, and the resulting precipitate was filtered off, washed with water and methanol. The resulting solid was further purified by recrystallization in cold 1,4-dioxane to give the product the yellow solid. Yield: (4.6 g, 84%). ^{1}H NMR (400 MHz, DMSO-d_6) δ 8.13 (s, 2H), 7.79 (s, 1H), 7.38-7.31 (m, 4H), 6.81-6.74 (m, 4H), 5.31 (s, 4H).

1.1.4 Synthesis of anthracene-9,10-dicarbaldehyde (ADA)

anthracene-9,10-dicarbaldehyde (ADA) was synthesized according to the literature with slight modification.[4]

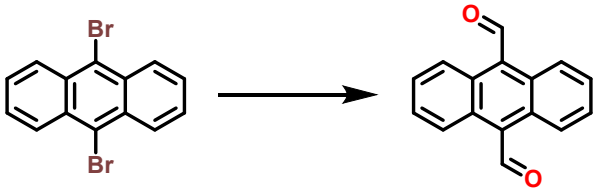

ADA

anthracene-9,10-dicarbaldehyde (ADA). A solution of 9,10-dibromoanthracene (1.0 g, 2.98 mmol) in anhydrous THF (25 mL) was cooled down to -78°C in a dry ice/acetone bath. 1.36 mL of n-butyllithium (3.27 mmol, 1.1 equiv.) were added dropwise to the solution and the mixture was stirred at -78°C for 1 hour. Next, 0.25 mL of anhydrous DMF (3.27 mmol, 1.1 equiv.) was added to the reaction mixture dropwise, and the mixture was brought to room temperature to stir for 30 minutes. After this time, the mixture was cooled to -78°C again and 3.4 mL of n-butyllithium (8.48 mmol, 2.85 equiv.) was added dropwise and left to stir at -78°C for 2 hours. Then, 1.15 mL of anhydrous DMF (14.85 mmol, 5.0 equiv.) was added dropwise and the mixture was brought to room temperature to stir for 1 hour. Finally, the reaction mixture was quenched by pouring into 25 mL water. The precipitate was filtered and dried to afford the title compound as an orange solid (0.33 g, 47.3%). ^{1}H NMR (600 MHz, chloroform-*d*) δ 11.47 (s, 2H), 8.72 (d, 4H), 7.69 (d, 4H).

1.1.5 Synthesis of 4,4'-(9,10-anthracenediyl) dibenzoic acid (DPA).

4,4'-(9,10-anthracenediyl) dibenzoic acid (DPA) was synthesized according to the literature with slight modification.[5]

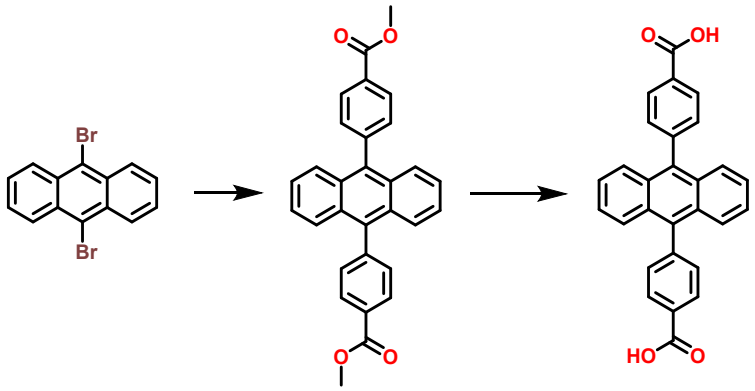

c DPA

Dimethyl-4,4'-(anthracene-9,10-diyl) dibenzoate (c). A mixture of 9,10- dibromo anthracene (1.8 g, 5.4 mmol), 4-methoxycarbonylphenylboronic acid (2.92 g, 16.2 mmol), CsF (3 g, 19.7 mmol), and $Pd(PPh_3)_4$ (0.17 g,0.15 mmol) was placed in a 150 mL two-necked flask and pumped for 15 min. 80 mL of degassed 1,2- dimethoxyethane was added through a cannula. The mixture was heated to reflux under ***an*** argon atmosphere for 72 h. After the mixture was cooled to room temperature, the solvent was removed. The yellow residue was suspended in water (40 mL) and extracted with CH_2Cl_2. After drying the mixed organic phase over $MgSO_4$ and removing the solvent, the crude product was purified by column chromatography (silica, CH_2Cl_2) to give the pure product of a yellow powder. ^{1}H-NMR (400 MHz, chloroform-*d*) δ 4.03 (s, 6H), 7.36 (m, 4H), 7.60 (m, 8H), 8.30 (d, 4H).

4,4'-(9,10-anthracenediyl) dibenzoic acid (DPA). 9,10-bis(p-(4-methoxycarbonyl)phenyl)anthracene (0.51 g, 1.15 mmol) was dissolved in 90 mL mixture of THF and MeOH (v/v = 2:1), 20 mL of a 20% KOH aqueous solution was added. The mixture was stirred to reflux for 12 h. the organic phase was removed under reduced pressure and the resulting suspension was diluted with 20 ml water. The precipitate formed by acidification with diluted hydrochloric acid was filtered and washed with water several times. ^{1}H-NMR (400 MHz, DMSO-d_6) δ 7.47 (m, 4H), 7.50 (d, 4H), 7.61 (m, 4H), 8.22 (d, 4H), 13.17 (s, 2H).

1.2 Synthesis of the materials. DPA-MOF was synthesized according to the literature with slight modification.[7] Typically, DPA (20.9 mg, 0.05 mmol), $ZrOCl_2 \cdot 8H_2O$ (10 mg, 0.03 mmol) and benzoic acid (100 mg, 0.82 mmol) in 5.0 mL of N,N-dimethyformamide (DMF) were ultrasonically dissolved in a 20 mL round-bottom flask. The mixture was stirred (650 rpm) at 100℃ for 40 min. After the reaction was done, DPA-MOF was collected by centrifugation (8000 rpm, 3 min) followed by washing with fresh DMF 3 times to afford the product as a white solid (2.2 mg, 42%).

1.3 Blank control. 2 mg **NKCOF-14** was dispersed in 20 mL ethanol in a vial and sonicated for 30 min to provide a mixture solution. Then the solution was irradiated by a 660 nm light with oxygen purged constantly. The fluorescence spectra were tested every 5 min with an excitation wavelength of 365 nm.

1.4 Singlet oxygen release through NKCOF-14-O. The resulting **NKCOF-14-O** was put into a 20 mL glass vial and heated to 100℃ for at least 1 h. After cooling to room temperature, **NKCOF-14** was collected for later testing.

1.5 Singlet oxygen capture and release through the model compound. 5 mg model compound (molecular weight: Cal. 536 g/mol, found: 537 [M+H]) and 0.5 mg methylene blue were mixed and dispersed in 10 mL $CDCl_3$. The mixture was sonicated for 20 min and irradiated by a 660 nm light with oxygen purged constantly. The solution gradually became homogeneous with the reaction time extended. After the reaction was finished, the solution was filtered through the filter (inside membrane pore width = ~0.22 μm) to remove the methylene blue. Then the resulting product was collected through vaporing the solvent to afford a light yellow solid (molecular weight: Cal. 568 g/mol, found: 569 [M+H]). For the oxygen release application, the product was put into a 10 mL round-bottom flask and heated to 100℃ for 2 h, then tested the H-NMR spectra to confirm the occurrence of the reaction.

1.6 Experiments to verify the released oxygen was in its excited state. **NKCOF-14-O** (10 mg) were dispersed in 15 mL DMF in a 20 mL vial. After sonicated for 20 min, 0.2 mg 1,3-Diphenylisobenzofuran (DPBF) was added and further sonicated for 10 min to dissolve. Then the solution was heated to 100℃ in the dark and tested the UV-Vis spectra after 1 h. The color of the solution was gradually changed from yellow to colorless with the reaction time extended, which indicated that the DPBF has bound with the released singlet oxygen.

Blank control. To further confirm the DPBF was reacted with the singlet oxygen, a blank control experiment was conducted. 0.2 mg DPBF was put into 15 mL DMF to make the homogeneous solution and heated to 100℃ for 1 h. The color of this solution was maintained and the absorbance of UV-Vis spectra was not change.

1.7 Experiments of making the thermal-responsive invisible ink for anti-fake application. 0.5 mg **NKCOF-14-O** was dispersed in 20 mL ethanol and sonicated for 30 min. The colorless mixture was then coated on the surface of a piece of the TLC slide with the letters N and K (NK = Nankai). The letters were invisible both in sunlight and 365 nm light after dried. And then the slide was heated to 100℃ for 1 h. The letters were visible at 365 nm light due to the reformation of the anthracene.

1.8 Pore size calculation of NKCOF-14 from the simulated structure. The simulated structure of **NKCOF-14** was input into Poreblazer software[6] to calculate the pore

limiting diameter. After the calculation, excellent agreement between the experimental and simulated values was achieved.

Table S1. Comparing the pore size from the experimental and simulated models.

	NKCOF-14
Experimental pore diameter (nm)	1.1
Simulated pore limiting diameter (nm)	1.1

1.9 Structure Simulation. Structural models were obtained from Reticular Chemistry Structure Resource (http://rcsr.anu.edu.au). Considering the geometry of building blocks, we assume that **NKCOF-14** possessed interpenetrated diamond structures. Structure models with different degrees of interpenetration were constructed, the calculated powder patterns were obtained from Reflex modules, which were used to compare with experimental PXRD patterns and determine the degrees of interpenetration. Once the periodical structures with specific topology were determined, the space group symmetry of these models was then reduced to allow the rotation of the anthracene rings. The piecewise constructed structure was fully optimized by Forcite module using Universal Force Field (UFF). For **NKCOF-15**, structure model was built in *P*1 symmetry and optimized.

2.0 Calculation of the actual $^1O_2$ loading in NKCOF-14. According to the XPS data displayed in Figure S13, the O atom percentage was increased from 6.22% to 10.79%. The molecular formula of **NKCOF-14** and **NKCOF-14-O** could be simplified as $(TMSFTA(ANT)_2)_n$ $(C_{86}H_{60}N_4O_4)_n$ and $(TMSFTA(ANTO_2)_2)_n$ $(C_{86}H_{60}N_4O_8)_n$. The

theoretic percentage of the O atom was ~4.25% and ~8.16%, respectively. Thus, the actual $^1O_2$ loading could be calculated to ~90% (10.79%/(6.22%*(8.16%/4.25%))).

2. Figures and Tables.

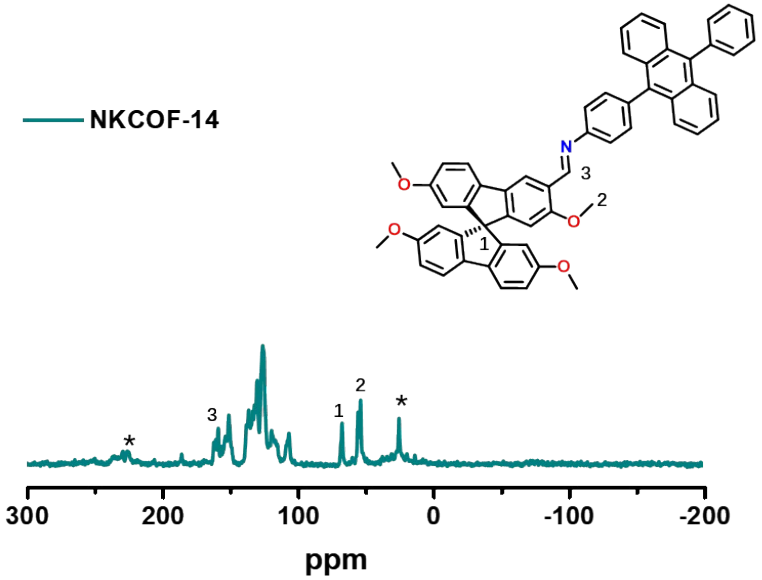

Fig. S1. Solid-state ^{13}C NMR spectra of **NKCOF-14**.

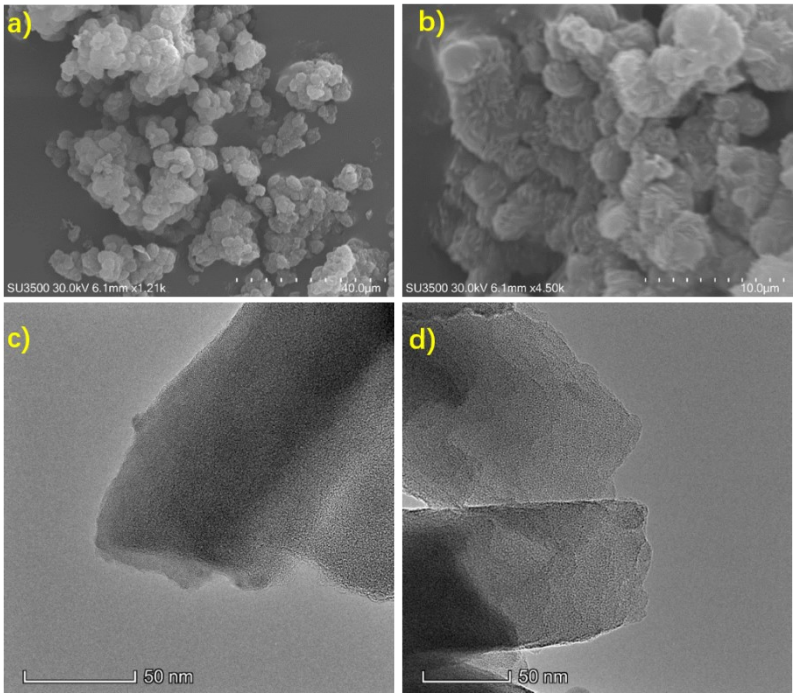

Fig. S2. (a, b) SEM images of **NKCOF-14.** (c, d) TEM images of **NKCOF-14.**

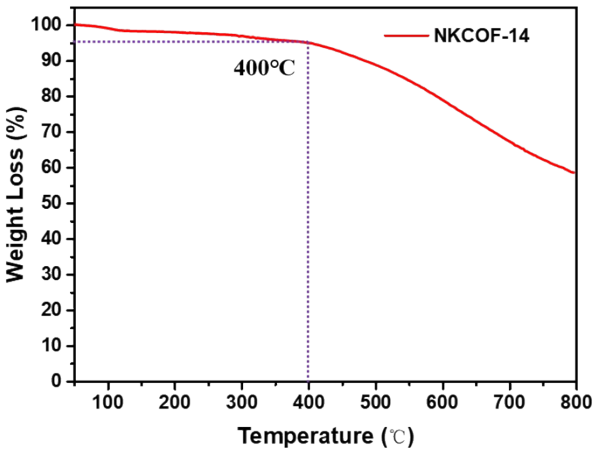

Fig. S3. TGA curve of **NKCOF-14**.

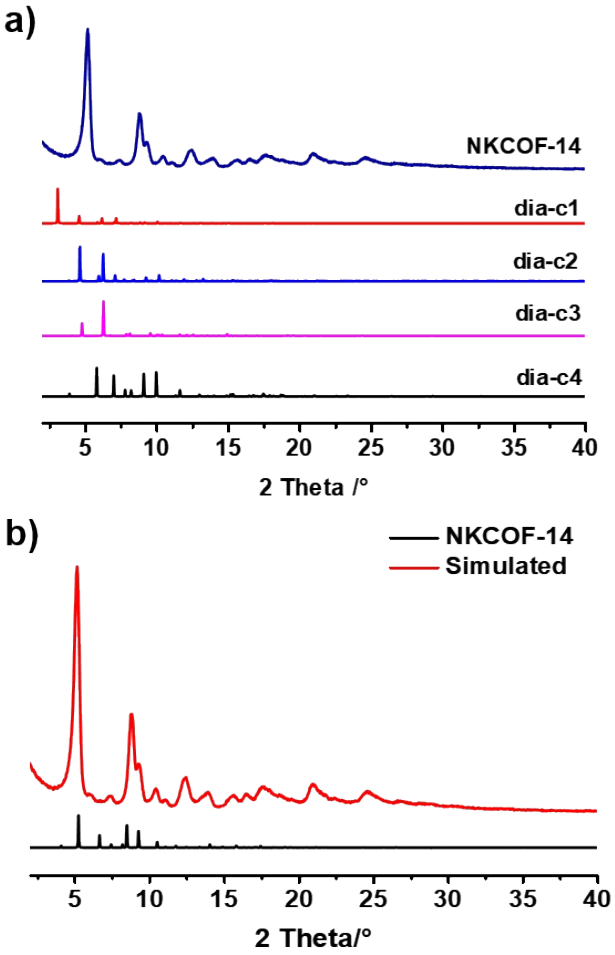

Fig. S4. (a) PXRD patterns of **NKCOF-14** and simulated patterns with different degrees of interpenetration. (b) PXRD patterns of **NKCOF-14** and simulated patterns after minor corrections.

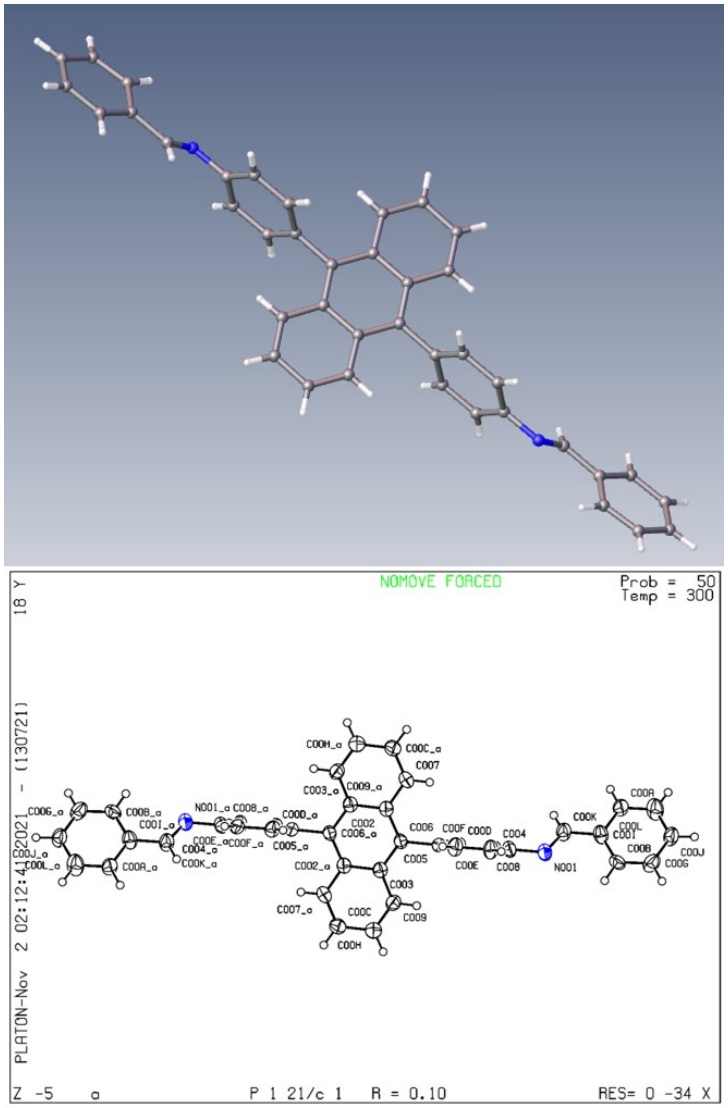

Fig. S5. Crystal structure of the model compound acquired from the single-crystal data.

Table S2. Single crystal data of the model compound.

	Model compound
Formula	$C_{40}H_{28}N_2$
CCDC number	2119654
Crystal system	monoclinic
Space group	P21/c
a/Å	15.1100(16)
b/Å	7.7907(7)
c/Å	12.0777(14)
α/°	90°
β/°	102.638(11)°
γ/°	90°
Volume/Å3	1387.3(3)
Z	6

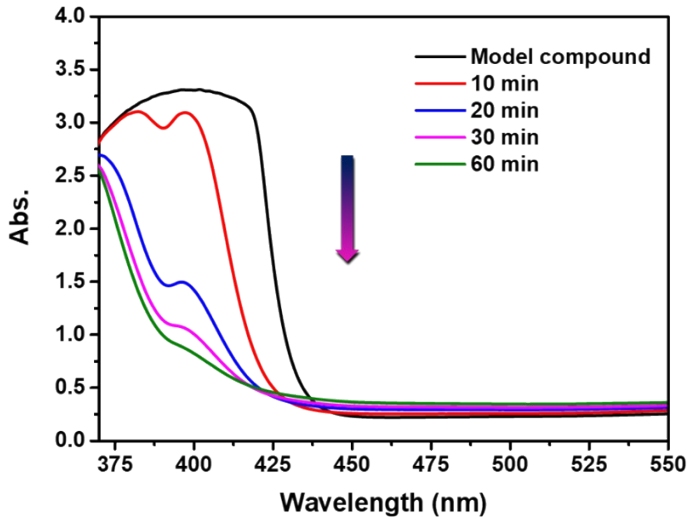

Fig. S6. UV-Vis spectra of the model compound and after cycloaddition with singlet oxygen with the reaction time extended.

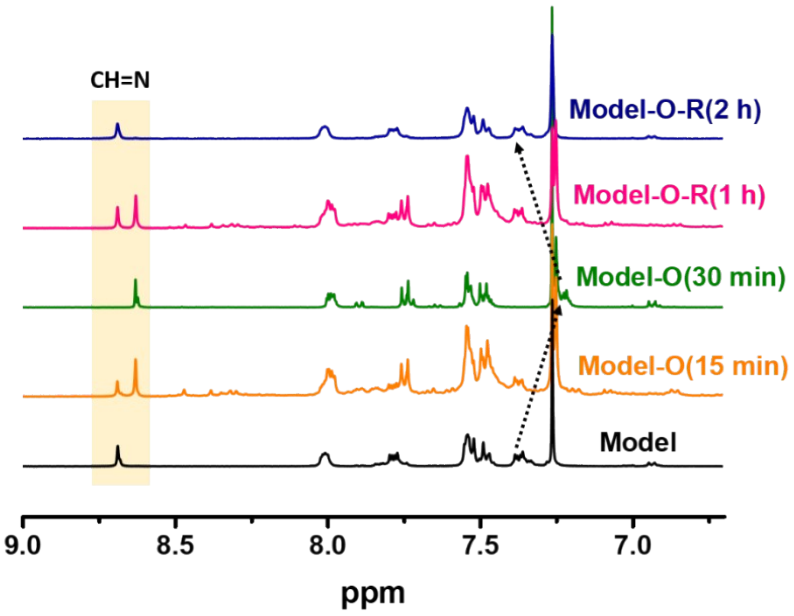

Fig. S7. ^{1}H-NMR spectra of one cycle of the model compound capturing and releasing singlet oxygen with the reaction time extended (Model-O represented for the oxygenation of the model compound; Model-O-R represented for the compound after releasing oxygen from Model-O, the spectra of the Model-O-R could be fully recovered to the spectra of the Model one).

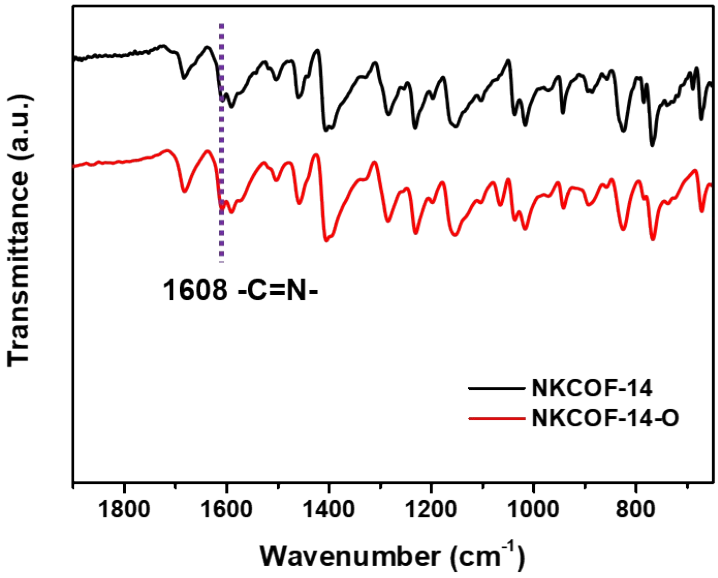

Fig. S8. FT-IR spectra of **NKCOF-14** and **NKCOF-14-O.**

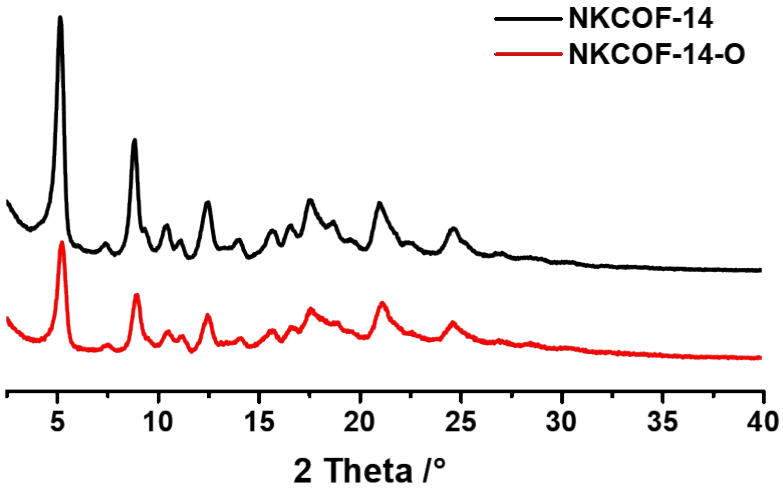

Fig. S9. PXRD patterns of **NKCOF-14** and **NKCOF-14-O.**

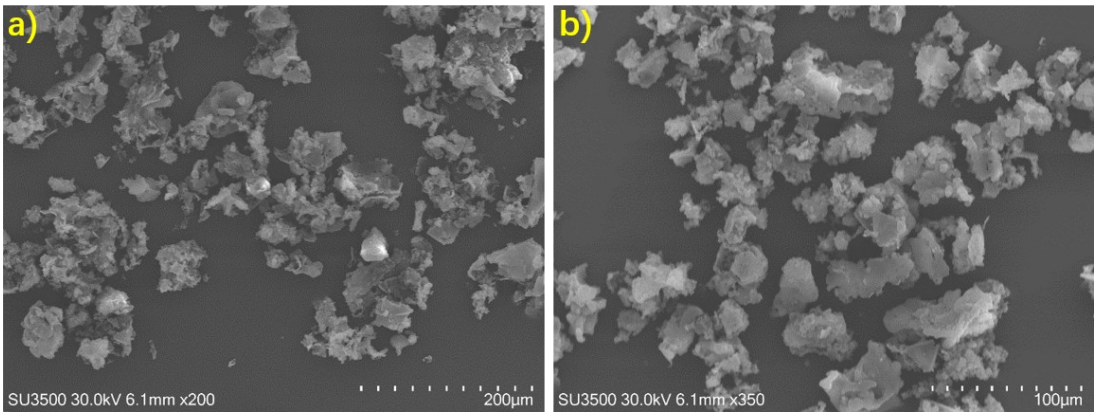

Fig. S10. SEM images of (a) **NKCOF-14**, (b) **NKCOF-14-O.**

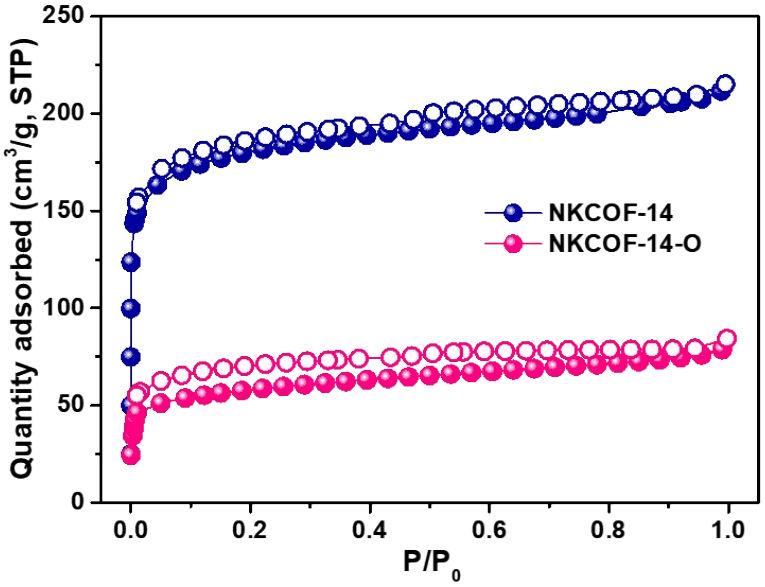

Fig. S11. N_2 sorption isotherms of **NKCOF-14** and **NKCOF-14-O.**

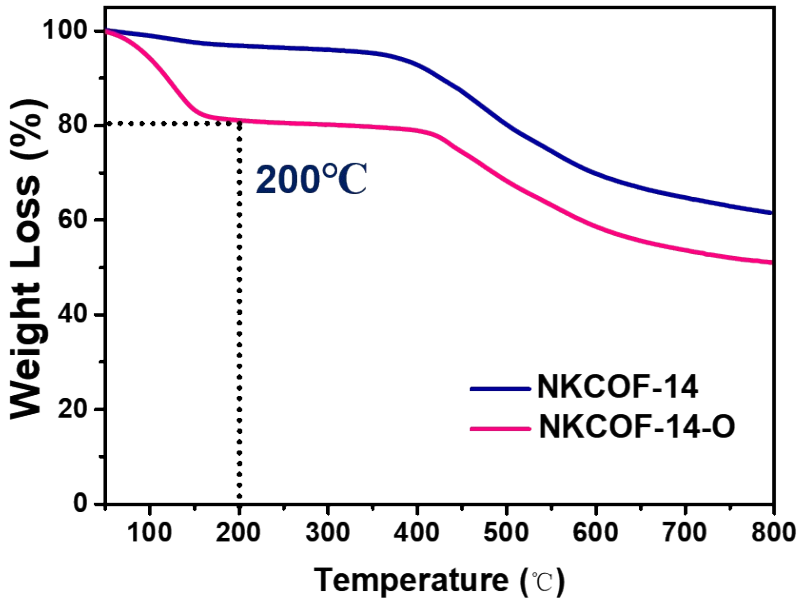

Fig. S12. TGA curves of **NKCOF-14** and **NKCOF-14-O.**

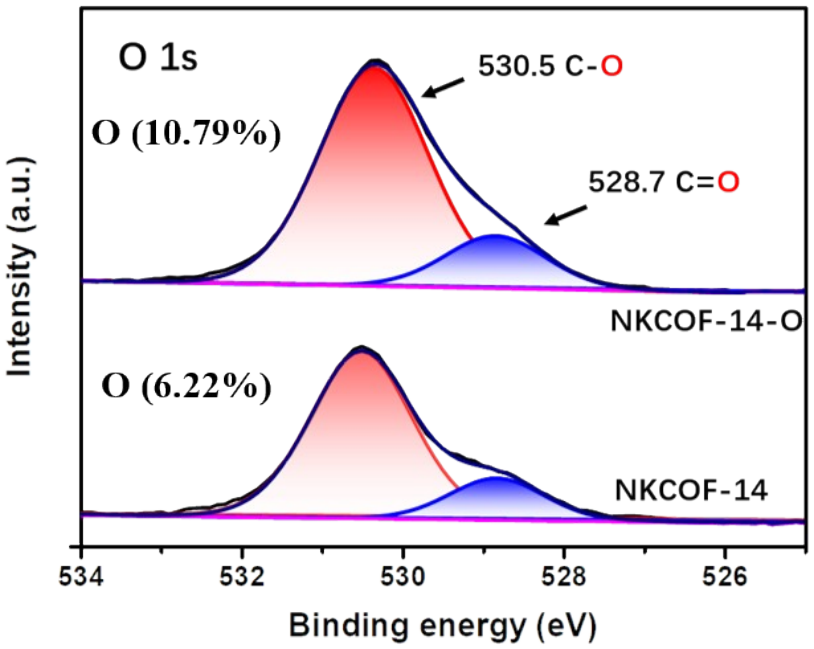

Fig. S13. XPS spectra of **NKCOF-14** and **NKCOF-14-O** (O 1s) (6.22% and 10.79% represented for the O element atom percentage of **NKCOF-14** and **NKCOF-14-O**).

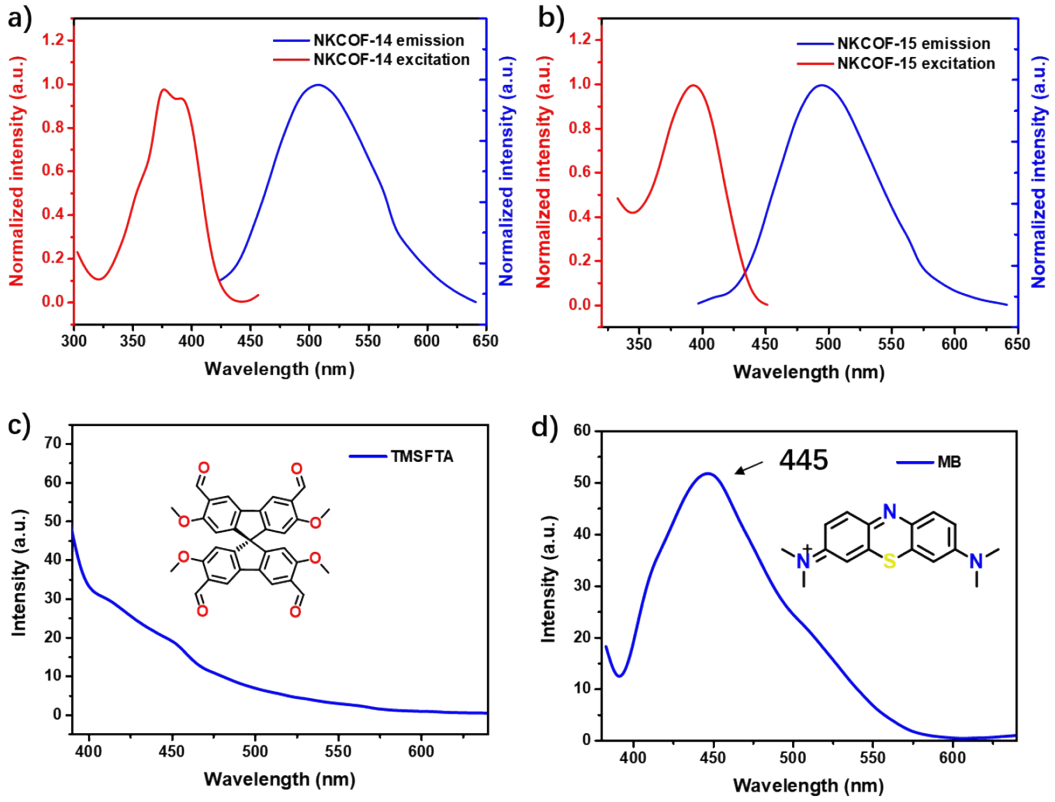

Fig. S14. Normalized excitation and emission spectra of (a) **NKCOF-14**, (b) **NKCOF-15.** (d, e) Emission spectra of the linkers (excitation: 365 nm).

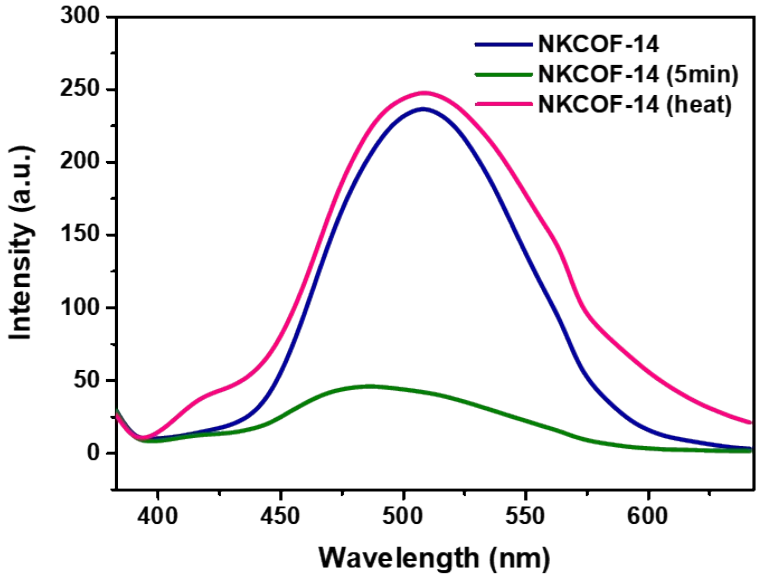

Fig. S15. Fluorescence spectra of **NKCOF-14** and after capture and release $^1O_2$.

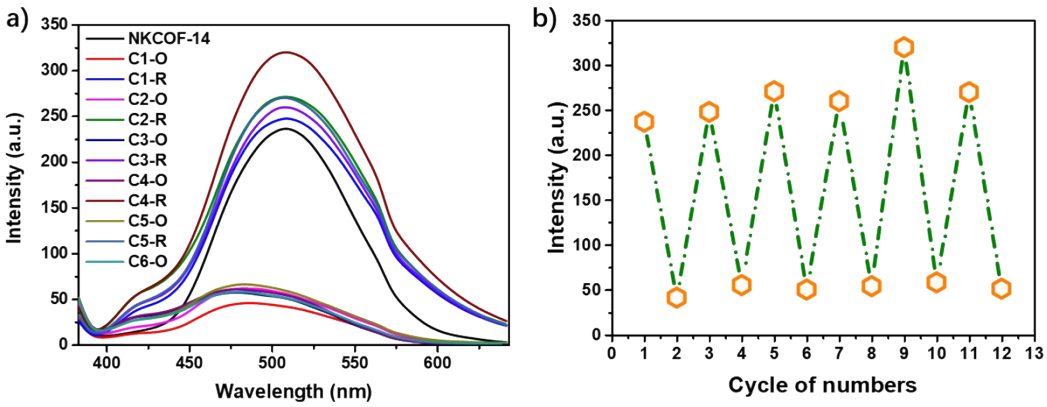

Fig. S16. (a) Fluorescence spectra of cycles of **NKCOF-14** capture and release singlet oxygen. (b) Recurring multiple cycles of the cycloreversion of **NKCOF-14.**

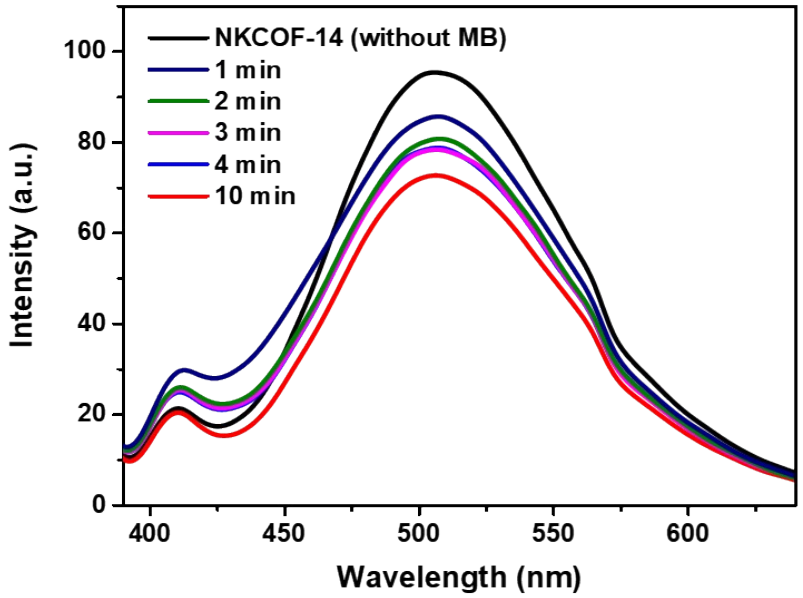

Fig. S17. Fluorescence spectra of **NKCOF-14** capture singlet oxygen without adding methylene blue.

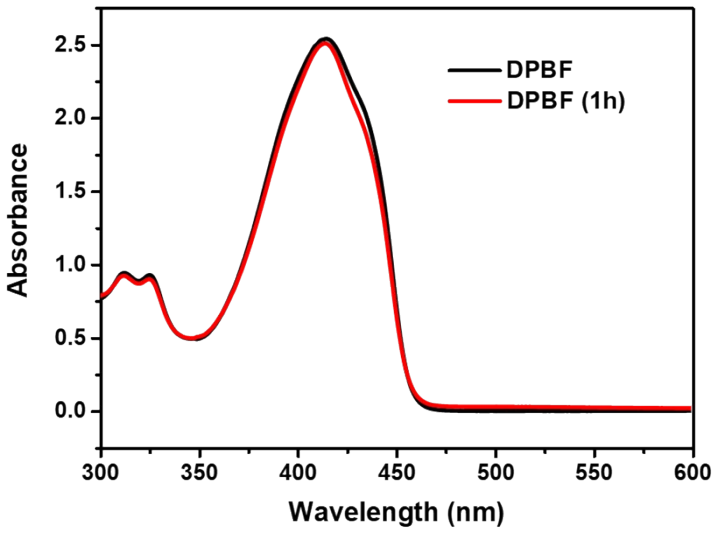

Fig. S18. UV-Vis spectra of the DPBF dissolved in DMF before and after heating to 100℃ for 1 h.

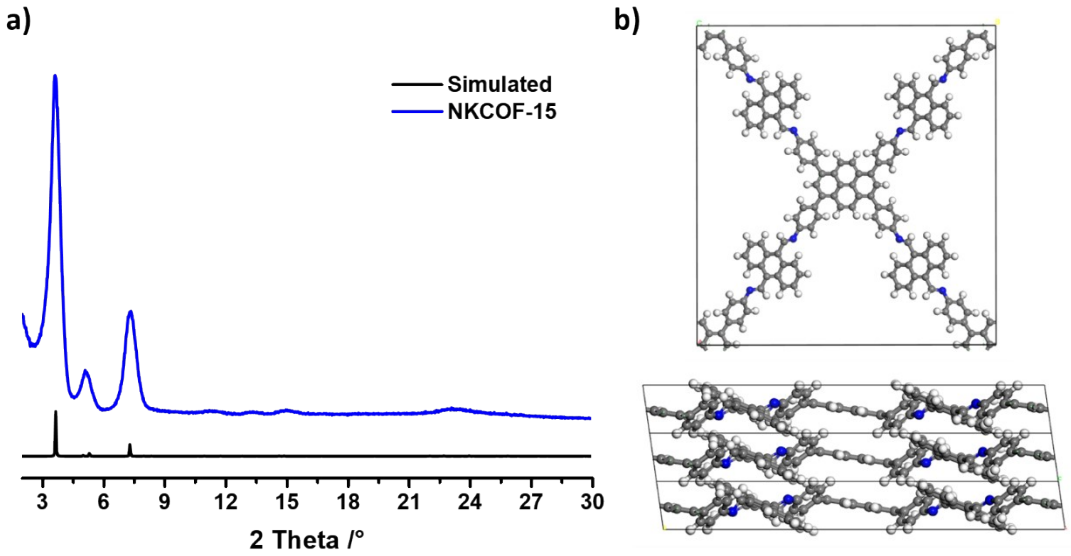

Fig. S19. (a) PXRD pattern of the **NKCOF-15**. (b) Simulated AA-stacking mode from the top view (top) and side view (bottom).

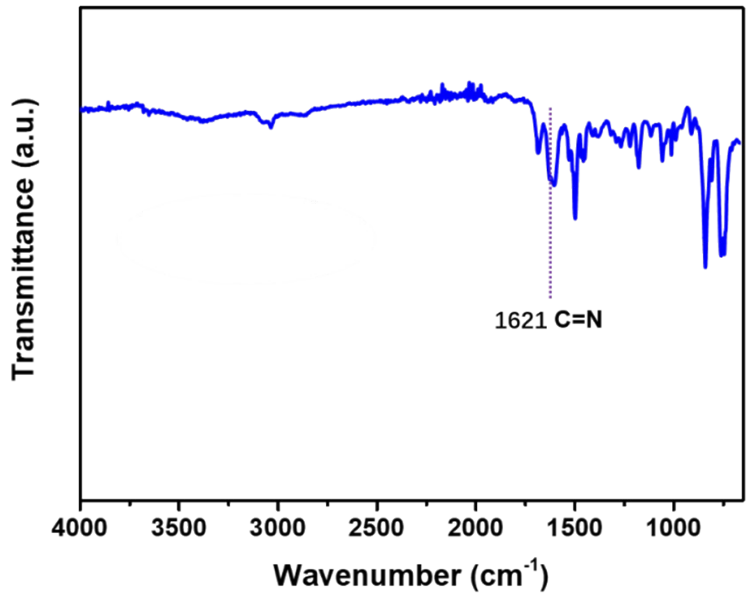

Fig. S20. FT-IR spectrum of **NKCOF-15.**

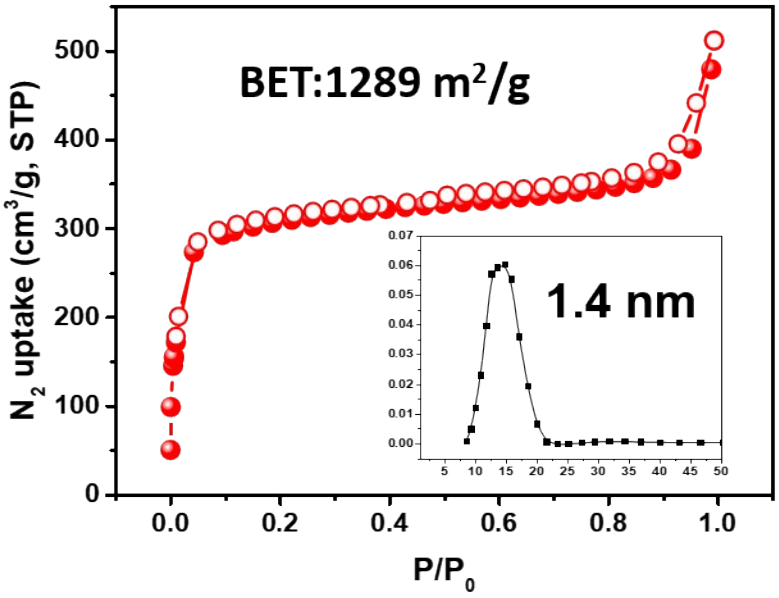

Fig. S21. N_2 sorption isotherms and pore size distribution of **NKCOF-15**.

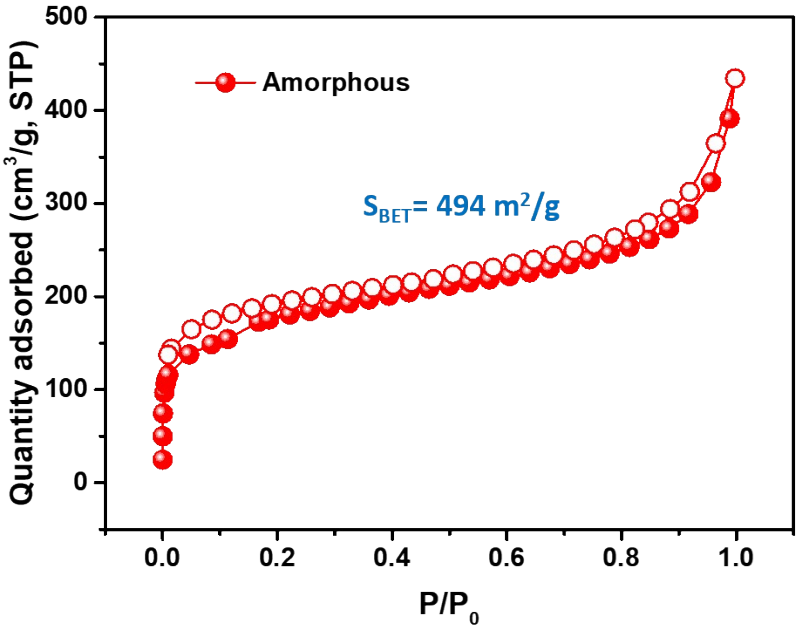

Fig. S22. N_2 sorption isotherms of the amorphous polymer.

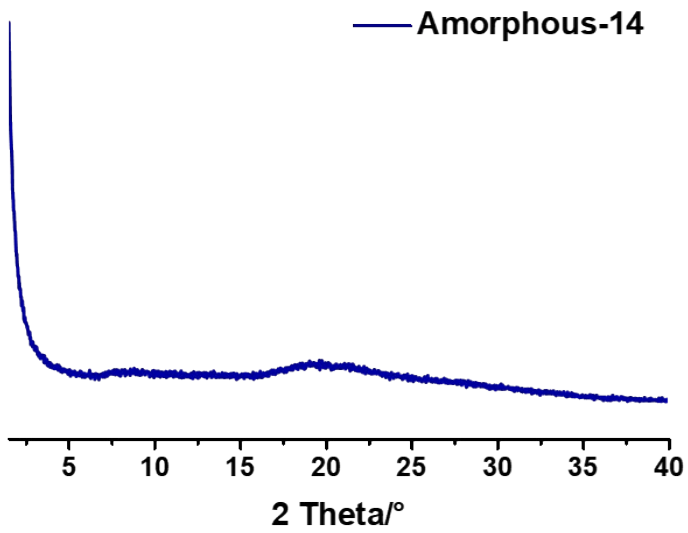

Fig. S23. PXRD pattern of the amorphous polymer.

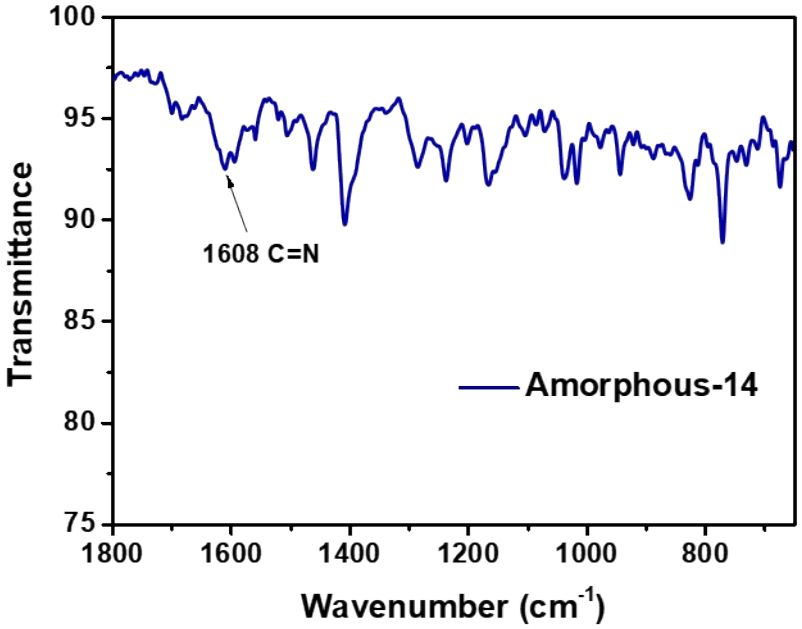

Fig. S24. FT-IR spectrum of the amorphous polymer.

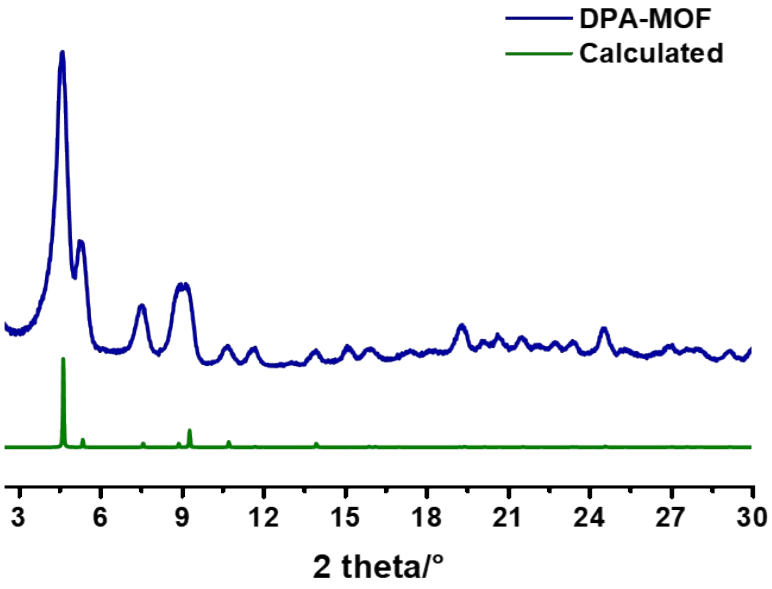

Fig. S25. PXRD pattern of the DPA-MOF and the calculated one.

Table S3. $^1O_2$ capture rates for various reported porous materials.

Materials	BET (m^2/g)	**$^1O_2$ capture rate**	Ref.
NKCOF-14[a]	**681**	**~80% at 5 min**	**This work**
NKCOF-15 [a]	1289	~38% at 20 min	This work
Amorphous-14 [a]	494	~60% at 20 min	This work
DPA-MOF [a]	1711	~63% at 20 min	This work
		~66% at 20 min	7
JUC-575 [a]	343	~14% at 20 min	8
JUC-576 [a]	246	~25% at 20 min	8
P1[b]	n/a	~50% at 20 min	9
Cage 2a[b]	n/a	~70% at 30 min	10
M1[b]	n/a	~55% at 30 min	11
COP-1[b]	n/a	~11% at 30 min	12
MOMF-1[c]	n/a	100% conversion at 120 min	13

[a]determined by Fluorescence quenching/enhancing rate

[b]determined by UV-Vis quenching rate

[c]determined by solution NMR spectra

(According to the listed materials above, there were usually three methods to confirm the $^1O_2$ capture rate. We considered that if the material could be dissolved in common solvents (e.g., DMF, $CHCl_3$), NMR techniques could be more accurate. However, most of the porous materials could not be dissolved in common solvents, emission, and UV-Vis techniques would be more convenient. The materials were dispersed in the solvents

and then tested with the real-time intensity of the spectrum to analyze and calculate the $^1O_2$ capture rate.)

Fig. S26. Photograph of the TLC slide whose surface was written letters N and K and after drying and stand for 7 days at 365 nm light irradiation.

Table S4. Unit cell parameters and fractional atomic coordinates for **NKCOF-14** calculated based on 4-fold interpenetrated **dia** net.

Space Group	P_4/n (No. 85)		
Calculated unit cell	a = b = 21.5762 Å, c = 22.6014 Å and α = β = γ = 90°		
Atom	x	y	z
C1	0.81625	0.60962	0.42662
C2	0.18906	1.32685	0.41664
C3	0.21959	1.28796	0.45781
C4	0.08352	0.70815	0.47780
C5	0.87921	1.26189	0.51929
C6	0.81466	1.25534	0.51007
C7	0.13957	0.88464	0.65561
C8	0.16515	0.85914	0.60421
N9	0.11756	0.88224	0.76116
C10	0.13029	0.86899	0.81601
C11	0.14457	0.85375	0.70983

C12	0.17417	0.79559	0.71181
C13	0.19953	0.76989	0.66036
C14	0.22333	0.77508	0.55216
C15	0.58255	0.58281	0.97136
C16	0.61359	0.61370	0.92463
C17	0.53806	0.53821	0.95790
C18	0.59862	0.59845	0.86505
C19	0.55314	0.55300	0.85286
C20	0.52378	0.52383	0.90006
O21	0.65937	0.65947	0.93475
C22	0.30177	1.30455	0.60649
C23	0.32503	1.32481	0.99441
C24	0.00000	1.00000	0.00000

Table S5. Unit cell parameters and fractional atomic coordinates for **NKCOF-14** calculated after minor correction and Pawley refinement.

Space Group	P_4/n (No. 85)		
Calculated unit cell	a = b = 23.4331 Å, c= 21.5619 Å and α = β = γ = 90°		
Atom	**x**	**y**	**z**
C1	0.80398	0.63009	0.40443
C2	0.19567	1.31113	0.40412
C3	0.22271	1.28007	0.45169
C4	0.10103	0.72308	0.45194
C5	0.86944	1.25002	0.49945
C6	0.80979	1.24962	0.50024
C7	0.14407	0.88785	0.64443
C8	0.17192	0.86161	0.59482

N9	0.10734	0.88755	0.75049
C10	0.11422	0.87438	0.80870
C11	0.13408	0.85852	0.69978
C12	0.15019	0.80148	0.70403
C13	0.17788	0.77521	0.65451
C14	0.22032	0.77762	0.54849
C15	0.57917	0.57071	0.97046
C16	0.60894	0.59763	0.92188
C17	0.53653	0.53264	0.95583
C18	0.59448	0.58541	0.85910
C19	0.55100	0.54633	0.84558
C20	0.52287	0.52056	0.89491
O21	0.65291	0.63672	0.93311
C22	0.30533	1.31063	0.60003
C23	0.33185	1.35045	0.99586
C24	0.00000	1.00000	0.00000

Table S6. Unit cell parameters and fractional atomic coordinates for **NKCOF-15** calculated based on the AA-stacking mode.

Space Group	*P*1 (No. 1)		
Calculated unit cell	a = b = 35.2540 Å, c= 4.06480 Å and α = 81.9083, β = γ = 90°		
Atom	**x**	**y**	**z**
C1	0.06896	0.89351	0.37309
C2	0.09942	0.90548	0.15984
C3	0.13222	0.88195	0.16625
C4	0.13494	0.84568	0.38009

C5	0.10383	0.83247	0.58279
C6	0.07124	0.85631	0.58015
C7	0.46445	0.58214	0.61741
C8	0.46406	0.54129	0.56140
C9	0.28822	0.73686	0.50527
C10	0.28681	0.77360	0.63950
C11	0.32519	0.71685	0.47293
N12	0.33088	0.68059	0.62429
C13	0.25428	0.71952	0.40268
C14	0.42979	0.48082	0.47096
C15	0.56781	0.39316	0.37891
C16	0.59855	0.40477	0.16791
C17	0.63106	0.38079	0.17586
C18	0.63318	0.34427	0.38759
C19	0.60172	0.33146	0.58789
C20	0.56950	0.35582	0.58448
C21	0.96337	0.08129	0.60669
C22	0.96345	0.04039	0.55185
C23	0.78532	0.23368	0.49706
C24	0.78336	0.27052	0.62940
C25	0.82259	0.21422	0.46510
N26	0.82866	0.17800	0.61561
C27	0.75163	0.21565	0.39653
C28	0.92990	0.97943	0.46295
C29	0.92835	0.10623	0.60848
C30	0.89782	0.09432	0.82096
C31	0.86528	0.11822	0.81729
C32	0.86304	0.15509	0.61040

C33	0.89394	0.16771	0.40249
C34	0.92622	0.14348	0.40222
C35	0.53305	0.41853	0.37983
C36	0.53343	0.45939	0.43582
C37	0.71405	0.27073	0.56870
C38	0.71591	0.23389	0.43817
C39	0.67702	0.29035	0.60098
N40	0.66760	0.32135	0.38842
C41	0.74764	0.28904	0.66522
C42	0.56770	0.51985	0.52647
C43	0.42973	0.60754	0.61888
C44	0.39904	0.59601	0.83062
C45	0.36678	0.62033	0.82631
C46	0.36498	0.65723	0.61949
C47	0.39605	0.66947	0.41242
C48	0.42805	0.64482	0.41280
C49	0.03390	0.91837	0.37447
C50	0.03379	0.95928	0.42904
C51	0.21753	0.77505	0.57701
C52	0.21884	0.73838	0.44352
C53	0.18081	0.79515	0.61177
N54	0.16934	0.82288	0.37797
C55	0.25137	0.79267	0.67564
C56	0.06734	0.02023	0.51778
C57	0.92976	0.89249	0.37178
C58	0.89913	0.90406	0.15948
C59	0.86682	0.87984	0.16377
C60	0.86493	0.84297	0.37090

C61	0.89596	0.83064	0.57815
C62	0.92801	0.85522	0.57792
C63	0.53389	0.58174	0.61723
C64	0.53385	0.54089	0.56126
C65	0.71662	0.72657	0.41654
C66	0.71835	0.76332	0.54842
C67	0.67968	0.70684	0.38395
N68	0.66931	0.67742	0.60812
C69	0.75024	0.70845	0.31893
C70	0.56750	0.48004	0.47077
C71	0.42862	0.39396	0.37935
C72	0.39799	0.40584	0.16803
C73	0.36530	0.38214	0.17562
C74	0.36301	0.34548	0.38528
C75	0.39410	0.33275	0.59059
C76	0.42653	0.35681	0.58702
C77	0.03280	0.08175	0.60675
C78	0.03324	0.04086	0.55204
C79	0.21206	0.23258	0.45656
C80	0.21496	0.26938	0.58764
C81	0.17442	0.21378	0.42992
N82	0.16746	0.17866	0.59745
C83	0.24515	0.21376	0.35353
C84	0.06760	0.98039	0.46298
C85	0.06753	0.10712	0.60763
C86	0.06940	0.14420	0.39894
C87	0.10170	0.16850	0.39448
C88	0.13286	0.15603	0.59962

C89	0.13073	0.11952	0.81117
C90	0.09818	0.09559	0.81964
C91	0.46361	0.41894	0.37996
C92	0.46364	0.45979	0.43594
C93	0.28422	0.26832	0.51792
C94	0.28130	0.23152	0.38640
C95	0.32186	0.28718	0.54348
N96	0.32832	0.32299	0.38648
C97	0.25112	0.28702	0.62244
C98	0.42999	0.52063	0.52677
C99	0.56890	0.60670	0.61808
C100	0.59952	0.59477	0.82960
C101	0.63227	0.61837	0.82167
C102	0.63477	0.65476	0.60888
C103	0.60343	0.66796	0.40868
C104	0.57094	0.64399	0.41213
C105	0.96446	0.91789	0.37401
C106	0.96400	0.95879	0.42886
C107	0.78774	0.76388	0.48768
C108	0.78590	0.72710	0.35449
C109	0.82491	0.78356	0.51826
N110	0.83072	0.81979	0.36708
C111	0.75401	0.78171	0.58958
C112	0.92963	0.01929	0.51754
C113	0.49928	0.60109	0.65095
C114	0.49864	0.47999	0.46527
C115	0.99797	0.10071	0.63948
C116	0.99875	0.97946	0.45786

C117	0.49823	0.39958	0.34631
C118	0.49885	0.52069	0.53182
C119	0.99931	0.89894	0.34160
C120	0.99848	0.0202	0.52309
C121	0.81643	0.28911	0.73439
C122	0.81426	0.32498	0.86921
C123	0.77931	0.34303	0.90422
C124	0.74629	0.32538	0.80396
C125	0.68261	0.21501	0.34199
C126	0.68456	0.17952	0.20153
C127	0.71955	0.16230	0.15140
C128	0.75278	0.18010	0.24631
C129	0.81901	0.70867	0.24861
C130	0.81694	0.67281	0.11342
C131	0.78205	0.6546	0.07922
C132	0.74899	0.6721	0.18042
C133	0.32016	0.79158	0.74557
C134	0.31853	0.82741	0.88146
C135	0.28385	0.84605	0.91590
C136	0.25057	0.82902	0.81433
C137	0.18526	0.72014	0.34606
C138	0.18666	0.68467	0.20484
C139	0.22138	0.66683	0.15556
C140	0.25487	0.68400	0.25193
C141	0.18235	0.28869	0.69346
C142	0.18537	0.32422	0.83225
C143	0.22077	0.34103	0.87243
C144	0.25335	0.32267	0.77067

C145	0.31386	0.21233	0.27820
C146	0.31081	0.17669	0.14105
C147	0.27544	0.15961	0.10519
C148	0.24291	0.17789	0.20843
C149	0.68500	0.78204	0.64521
C150	0.68684	0.81750	0.78614
C151	0.72177	0.83486	0.83601
C152	0.75505	0.81723	0.74028

3. References.

1. S. Ghosh, A. Nakada, M. A. Springer, T. Kawaguchi, K. Suzuki, H. Kaji, I. Baburin, A. Kuc, T. Heine, H. Suzuki, R. Abe and S. Seki, Identification of Prime Factors to Maximize the Photocatalytic Hydrogen Evolution of Covalent Organic Frameworks, *J. Am. Chem. Soc.,* 2020, **142**, 9752-9762.

2. a) J. Pang, M. Wu, J.-S. Qin, C. Liu, C. T. Lollar, D. Yuan, M. Hong and H.-C. Zhou, Solvent-Assisted, Thermally Triggered Structural Transformation in Flexible Mesoporous Metal–Organic Frameworks., *Chem. Mater.,* 2019, **31**, 8787-8793. b) L. Pop, F. Dumitru, N. D. Hădade, Y.-M. Legrand, A. van der Lee, M. Barboiu and I. Grosu, Exclusive Hydrophobic Self-Assembly of Adaptive Solid-State Networks of Octasubstituted 9,9′-Spirobifluorenes., *Org. Letters.,* 2015, **17**, 3494-3497.

3. D. Yan, Z. Wang, P. Cheng, Y. Chen and Z. Zhang, *Angew. Chem. Int. Ed.,* 2021, **60**, 6055–6060.

4. E. Gonzalez-Rodriguez, M. A. Abdo, G. Dos Passos Gomes, S. Ayad, F. D. White, N. P. Tsvetkov, K. Hanson and I. V. Alabugin, Twofold pi-Extension of Polyarenes via

Double and Triple Radical Alkyne peri-Annulations: Radical Cascades Converging on the Same Aromatic Core, *J. Am. Chem. Soc.,* 2020, **142**, 8352-8366.

5. J.-Y. Zeng, X.-S. Wang, Y.-D. Qi, Y. Yu, X. Zeng and X.-Z. Zhang, Structural Transformation in Metal–Organic Frameworks for Reversible Binding of Oxygen, *Angew. Chem. Int. Ed.,* 2019, **58**, 5692-5696.

6. L. Sarkisov and A. Harrison, Computational structure characterisation tools in application to ordered and disordered porous materials, *Molecular Simulation*, 2011, **37**, 1248-1257.

7. J.-Y. Zeng, X.-S. Wang, Y.-D. Qi, Y. Yu, X. Zeng and X.-Z. Zhang, Structural Transformation in Metal-Organic Frameworks for Reversible Binding of Oxygen, *Angew. Chem. Int. Ed.,* 2019, **58**, 5692-5696.

8. M. Zhang, J. Fang, Y. Liu, Y. Wang, L. Liao, L. Tang, L. Zhu, S. Qiu and Q. Fang, 3D Covalent Organic Frameworks Based on Polycyclic Aromatic Hydrocarbons for Reversible Oxygen Capture, *Small Struct.,* 2021, **2**, 2000108.

9. C. H. Wang and E. E. Nesterov, Amplifying fluorescent conjugated polymer sensor for singlet oxygen detection, *Chem. Commun.,* 2019, **55**, 8955-8958.

10. C. Mongin, A. M. Ardoy, R. Mereau, D. M. Bassani and B. Bibal, Singlet oxygen stimulus for switchable functional organic cages, *Chem. Sci.,* 2020, **11**, 1478-1484.

11. Y. Q. He, W. Fudickar, J. H. Tang, H. Wang, X. Li, J. Han, Z. Wang, M. Liu, Y. W. Zhong, T. Linker and P. J. Stang, Capture and Release of Singlet Oxygen in Coordination-Driven Self-Assembled Organoplatinum(II) Metallacycles, *J. Am. Chem. Soc.,* 2020, **142**, 2601-2608.

12. H. Lai, J. Yan, S. Liu, Q. Yang, F. Xin and P. Xiao, Peripheral RAFT Polymerization on a Covalent Organic Polymer with Enhanced Aqueous Compatibility for Controlled Generation of Singlet Oxygen, *Angew. Chem. Int. Ed.,* 2020, **59**, 10431–10435.

13. M. Fujimura, S. Kusaka, A. Masuda, A. Hori, Y. Hijikata, J. Pirillo, Y. Ma and R. Matsuda, Trapping and Releasing of Oxygen in Liquid by Metal-Organic Framework with Light and Heat, *Small,* 2021, **17**, e2004351.